J. Condensed Matter Nucl. Sci. 13 (2014) 528–542

Research Article

Energy Gain From Preloaded ZrO_2–PdNi–D Nanostructured CF/LANR Quantum Electronic Components

Mitchell R. Swartz*, Gayle Verner and Jeffrey Tolleson
JET Energy Inc., Wellesley Hills, MA 02481-0001, USA

Abstract

Previously, we reported that such nanocomposite ZrO_2–PdNiD LANR materials have been made into LANR/CF transistors which exhibit energy gain and simultaneous non-thermal near infrared emission. This is accompanied by complicated polarization/transconduction phenomena including an avalanche transconduction electrical breakdown, which has a critical role in excess heat generation. This paper presents a new generation of preloaded LANR (CF) activated nanocomposite ZrO_2–PdNiD CF/LANR quantum electronic devices capable of energy gain. These devices dry, glued into electrically conductive, sealed, configurations. The core is ZrO_2–(PdNiD) with additional D_2 and H_2. They are self-contained CF/LANR quantum electronic components containing ZrO_2–PdNi–D LANR/CF nanostructured materials which generate significant excess heat from applied electric fields. They also feature two terminals and self-contained superior handling properties enabling portability and transportability. Most importantly, the activation of the desired LANR reactions is, for the first time, separated from the loading of the substrate. Although their development has required control of their breakdown states and the quenching tendencies of nanostructured materials, these ZrO_2–PdNiD CF/LANR quantum electronic devices are potentially very useful because they are reproducible active nanostructured CF/LANR quantum electronic devices.
 ISSN 2227-3123

Keywords: Dry cold fusion, NANOR®, Preloading, ZrO_2PdNiD, ZrO_2PdD

1. Introduction

We report a new generation of LANR (CF) activated nanocomposite ZrO_2–PdNiD CF/LANR quantum electronic devices capable of significant energy gain [1]. Lattice assisted nuclear reactions (LANR) are also known as CF, CMNS, and LENR. These self-contained, two-terminal, CF/LANR quantum electronic components (NANOR®-type LANR devices) feature new composition, structure, and superior handling properties enabling portability and transportability. Most importantly, they are preloaded so that LANR activation is separated from loading. These devices contain active ZrO_2/PdD nanostructured material at their core. The preloaded nanocomposite LANR/CF materials are made into dry electronic circuit devices, which required surmounting their extremely high electrical resistances. They are then,

*E-mail: mica@theworld.com

 ISSN 2227-3123

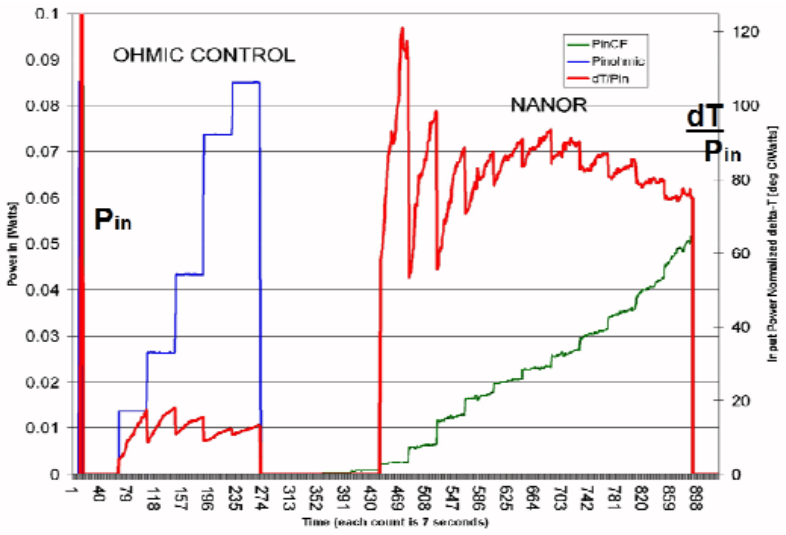

Figure 1. Input Power and Resulting Output Temperature rise (normalized to input electrical power) of a self-contained CF/LANR quantum electronic component , a Series V two terminal NANOR®-type device containing active preloaded ZrO_2/PdNiD nanostructured material at its core. These curves plot the temperature rise normalized to input electrical power as a function of time.

remotely, easily activated, driven by an electrical circuit and controlled by an electrical driver (cf. Figs. 1,3–5). They have been carefully evaluated for energy gain, including during, and after, the January, 2012 IAP MIT Course on CF/LANR (Figs. 3,4; [1]). That calorimeter had parallel diagnostics, such as heat flow measurement, and calibration including an ohmic (thermal) control located next to the NANOR®.

This demonstrates that these NANORs can be fashioned into completely preloaded easily activated LANR (CF) Integrated Circuits which enable an entire new generation of ZrO_2–PdNiD preassembled IC electronic devices. The importance is they enable LANR devices and their integrated systems to now be fabricated, transported, and then activated. They *are* the future of clean, efficient energy production.

2. Background

Clean energy production is critically important today, and in the foreseeable future, from whatever source. LANR use hydrogen-loaded alloys to create heat and other reactions. They are an energy multiplier because the energy density of LANR reactions is ten million times that of gasoline. LANR will play a critical role in all future technologies with potential revolutionary applications to all energy issues – robotics, transportation, electricity production, artificial internal organs, and space travel [2]. In the case of LANR, there can rarely occur, in a lattice under special conditions, the fusion of two heavy hydrogen nuclei to form a helium nucleus at near room temperature. The product helium-4, or simply helium, is *de novo* meaning that this helium is created new and fresh, generated directly from two, driven by more, deuterons physically located within the loaded palladium, nickel or one of their nanostructured materials. These reactions were first reported in aqueous. Today, they involve a palladium-alloyed lattice or nanomaterials where the process occurred irregularly at low efficiency. Most importantly, the product with LANR, helium, is environmentally safe and does not produce global contamination or warming. We previously demonstrated success in LANR aqueous

systems, linked to high solution resistance (impedance) and shaped-metamaterial PHUSOR®-type LANR devices, with power gains more than 200–500%; and short term power gains using codepositional high impedance devices DAP (Dual anode Phusor®-Type LANR device; Pd/D_2O, Pd$(OD)_2$/Pt–Au have reached ∼8000% compared to input energy and to input energy transferred to control dissipative devices (100%) [3–8]. However, successful LANR requires engineering of multiple factors including loading, adequate confinement time (sometimes weeks to generate vacancies in non-nanomaterial systems), loading rate, and prehistory (with careful avoidance of contamination and materials and operational protocols which quench performance). Specifically, nanostructured materials, metamaterials, and their controlled operation improve success [9–11].

Nanostructured materials are important in LANR, and are also produced in codeposition structures [12], observed producing non-thermal near infrared emissions when active [13,14], and exhibiting LANR excess heat correlated with the size of the Pd–D nanostructures [6,7]. Relevant to LANR and the future of LANR devices, nanostructured materials offer great opportunity. As a result of the small size, nanotechnology built using these new nanostructured materials have two amazing properties. First, nanostructured materials have incredibly large surface area to volume ratios. Second, many also have new unexpected quantum mechanical properties. Nanostructured materials enable quantum confinements, surface plasmon resonances, and superparamagnetism. Examples of material properties which unexpectedly change by nanostructured utilization include significantly decreased melting temperatures (gold), significantly increased electrical conductivity (silicon), increased flammability (aluminum), improved catalytic properties (platinum), and unexpected transparency of metals (copper). Solvated gold nanoparticles have colors which range from red to black.

These nanostructured LANR materials include nanoparticles, nanocrystals, quantum dots, nanocatalysts. nanowires, nanocrystals, nanoclusters, nanodendrimers and higher polymer aggregates, and metallic-organic hybrids. They are made from metals, semiconductors, oxides, ceramics, polymers, composite materials, glasses, alloys and combinations of the above.

LANR devices use hydrogen-loaded alloys of nanostructured materials to create heat and other reactions. At LANR's nanostructured material "core" is an isotope of hydrogen, usually deuterons, which are tightly packed ("highly loaded") into the binary metals, alloys, or in this case, nanostructured compounds, containing palladium or nickel, loaded by an applied electric field or elevated gas pressure which supply deuterons from heavy water or gaseous deuterium. Loaded are isotopes of hydrogen -protons, protium, deuterons, deuterium, and hydrogenated organic compounds, deuterated organic compounds, D_2, H_2, deuterides and hydrides. Precisely for these NANOR®-type LANR devices, the fuel for the nanostructured material in the core, is deuterium.

Palladium nanoparticles often have a vacancy in their center. Similarly, LANR nanostructures include vacancies within them. In the alloys, they must drift into the bulk from the surface. This diffusion is slightly facilitated by the loading itself. *de novo* Pd–D vacancies have been made in loaded Pd (and Ni) with electron beam irradiation [15]. Codeposition has been used to make palladium, nickel and alloyed loaded materials on top of electrodes, and used dual anode LANR systems to produce very high levels of such LANR nanostructured materials locally. In addition, nanostructured materials have been used in LANR using palladium black [16] in a double structure (DS)-cathode. They reported more than 200 MJ of excess energy was continuously produced for over 3000 h at an average rate of 50–100 kJ/h. The DS-cathode is a Pd cathode with an internal vacuum zone filled with a deuterium storage type powder and an outer cylindrical vessel of Pd metal (wall thickness of 3 mm). Such bulk cathodes rely on diffusion, making it difficult to reach 100 at% concentration solid solution of D in Pd or the other nanostructured material. The D ions are postulated to move over the surfaces of the Pd black by the "spillover-effect", without the need to becoming D_2 molecules. Previously, we reported production of excess heat using nanomaterial palladium, nickel, and newer alloyed compounds, such as ZrO_2PdNi, and in a LANR transistor configuration, driven by two applied electric field intensities, which demonstrate LANR heat associated with low level near-infrared emission, controlled by two optimal operating point manifolds.

ZrO_2–(PdNi)–D LANR/CF nanostructured materials generate excess heat [3], including with acoustic and electric fields, and with additional significant effects from orthogonal applied DC magnetic field intensities [6]. There are complicated polarization/transconduction phenomena including an "avalanche (transconduction electrical breakdown) effect" which has a critical role in excess heat. The LANR nanostructured materials have been made into LANR/CF transistors [7] which exhibit energy gain and simultaneous non-thermal near infrared emission.

LANR materials and nanostructured materials, when active at their OOP, generate non-thermal near infrared (NT–NIR) emission. Dr. Stan Szpak (SPAWAR) et alia reported the emission of infra-red from LANR codeposition devices. However, they did not use a control or calibration. In 2008, Swartz demonstrated that two controls are needed, including normalization of NIR emission intensities to both non-energized background and to ohmic control areas; in experiments involving a variety of LANR metamaterial spiral-wound and other Phusor®-type lattice assisted nuclear reaction (LANR) systems, including high impedance palladium ($Pd/D_2O/Pt$,$Pd/D_2O/Au$), codepositional ($Pd/Pd(OD)_2/Pt$) heavy water, and nickel ($Ni/H_2O_xD_2O_{1-x}/Pt$,$Ni/H_2O_xD_2O_{1-x}/Au$)) light water Phusor-type LANR devices. Swartz demonstrated that the emission of near-IR from the electrodes coupled with LANR operation is only observed when active electrodes operated at their optimal operating point, and that there was a linkage of excess power gain and heat flow with simultaneous NT–NIR emission [13]. Most importantly, NT–NIR is coupled and specific to the LANR devices' excess heat production and not its physical temperature.

3. Experimental – Materials

We designed and prepared several generations of active LANR (CF) preloaded nanocomposite ZrO_2–PdNiD CF/LANR quantum electronic devices capable of significant, reproducible energy gain (Fig. 2). The preactivated LANR nanostructured material is incorporated into a proprietary self-contained CF/LANR quantum electronic component, called a two terminal NANOR®-type of LANR device. These feature two terminals and self-contained superior handling properties enabling portability and transportability. The Series V NANOR®-type LANR devices feature new structure and superior handling properties. Series VI NANOR®-type LANR devices augment that with new composition, and, most importantly, are preloaded so that LANR activation is separated from loading. The symbol N in a solid circle is used here to denote the active preloaded NANOR-type LANR device.

These are potentially very useful and more reproducible nanostructured CF/LANR quantum electronic devices, whose development has required control of their breakdown states and quenching tendencies. Most importantly, the activation of this cold fusion reaction is, for the first time, separated from its loading at room temperature [17,18]. As a result, these are called preloaded NANOR®-type nanocomposite LANR materials and devices. Generally speaking, nanostructure preparation, assembly, and driving are very complicated and there are several methods of each which will be briefly reviewed.

The NANOR®-type of LANR devices contain active nanostructured material in the core, which is ZrO_2–PdNiD, ZrO_2–Pd, ZrO_2–NiD, ZrO_2–NiH, ZrO_2–PdNiDAg, and the like, with the the atomic ratios being usually in the range of Zr (∼60–70%), Ni (0–30%), and Pd (0–30%) by weight, with the weights being before the oxidation step, and several later additional preparation steps. The additional D_2 and H_2 yield loadings (ratio to Pd) of up to more than 130% D/Pd. For simplicity, all of these nanostructured materials in the core, in their range of deuterations, will henceforth simply be referred to as ZrO_2–PdD, ZrO_2–NiHD, and ZrO_2–PdNiD.

For the NANOR-type LANR devices reported in this paper, although the nanostructured LANR material might be loaded with either hydride, at this time we have focused solely on D, and used experimental structures, paradigms, materials for that.

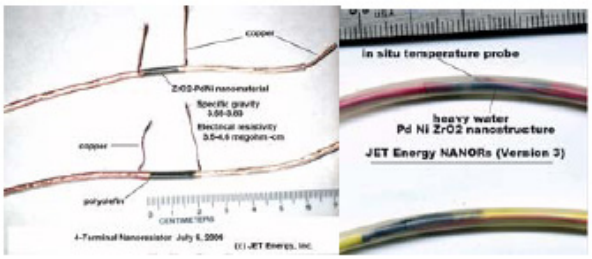

Figure 2. Series II and III two terminal NANOR®-type devices containing active ZrO_2–PdNiD nanostructured material at their core.

There are issues of particle size, electrical conductivity, potential contamination, and potential toxicity, that each must be discussed first. The size of nanostructured materials is key. The desired nanostructure islands of NiPdD have characteristic widths of 2–20 nm size. This nanostructure size is selected because it can react cooperatively, generating large amplitude, low frequency oscillations. The characteristic width is between 7 and 14 nm. These size structures tend to be Raman active, with the islands having anharmonic terahertz vibrations. Furthermore, the storage capacity decreases rapidly when the nanostructure size is greater 30 nm. It is not unreasonable to see rapid drop off in LANR success if sizes are larger than 20–30 nm. The vibrations of nanostructured materials are very important for activity. The nanostructured vibrational modes are maximized with softening of the material in which they are contained. It is reported that some of the modes are so large that they can cause a sudden structural phase change to a lower free energy state.

Preparation of active nanostructured materials, able to undergo preloading, requires very pure materials. Contamination remains a major problem, with excess heat potentially devastatingly quenched. Contaminants can appear from both electrode and container degradation and leeching, from atmospheric contamination, especially after temperature cycling. Furthermore, the heavy water and D_2 are hygroscopic, therefore must be kept physically isolated from the air by seals.

Potential toxicity must be considered. Nanostructured and nanocomposite materials have potential human and environmental health hazards. The large number of particles, and greater specific surface area, yield increased absorptive risk through the skin, lungs, and digestive tract. In 2008, the Karolinska Institute (Sweden) examined the impact of metallic nanoparticles on human lung epithelial cells. Ferric oxide nanoparticles produced the smallest amount of DNA damage and were relatively non-toxic. Titanium and zinc oxide nanoparticles were more toxic, and carbon nanotubes also produced DNA damage. Cupric oxide nanoparticles were the most toxic, and are avoided here.

The preloaded NANORs involve palladium as one of the elements within the zirconia nanostructured material. Palladium powder can be obtained (Goodfellow, Alpha Aesar) which usually present sizes from 60 to 200 nm. Most relevant is deuterided palladium-black, palladium black dual cathode, glass ZrO palladium-black systems, and a wide variety of other nanostructures.

Pd and Ni nanoparticles can be made by chemical solution deposition, also known as the solution–gelation (sol–gel) process, used in ceramic engineering for making metal oxides. The precursor substrates are metallic alkoxides and chlorides which polymerize by hydrolysis forming a colloidal suspension. Solvent removal controls hydration, shrinkage and porosity. The deposition method controls whether films (dip- or spin-coating), ceramics, glasses, fibers, membranes, aerogels, or powders result. The technologies began in 1880 when it was noted that tetraethyl orthosilicate in acid forms SiO_2 monolithic fibers.

Nanocrystalline palladium has been made by inert gas condensation and compaction with grain, crystallite, sizes ranging from 5 to 50 nm. Palladium nanodendrimers of ∼300 Pd atoms in a metallic core of 2.0 nm diameter are also fabricated with nearly 90% of the metal nanoparticle surface is unpassivated and available for catalysis. The dendrons inhibit metal agglomeration without adversely affecting chemical reactivity. Palladium nanoparticles and nanowires are also created by electrochemical deposition, usually on a carbon surface. Pd nanoparticles made on a gold surface show proton reduction catalytic activity enhanced by more than two orders of magnitude, as the diameter of the palladium particles decreases from 200 to 6 nm. As an alternative, there are the zirconium oxide binary and ternary Group VIII LANR materials. ZrO_2–PdNiD and ZrO_2–PdH are made by the initially by the Yamaura protocol and are used to store hydrogen gas for fuel cells. Arata used this powder for his LANR work. Today, second and third generation nanostructured powders, such as Zr 67% Ni 29% Pd 4% (by weight before the oxidation step), absorb a very large number of deuterons for each and every nickel and palladium nuclei. There are reports of numbers in the order of 3.5. Close up, in ZrO_2–PdNi–D LANR/CF nanostructured materials, the lattice of Pd is expanded by Zr. There are then also wrought other major changes by the oxidation of the Zr. The nanostructured material, ZrO_2–(Pd_xNi_{1-x}), is a composite distribution of nanostructured ferromagnetic "islands" separated among a vast dielectric zirconia "ocean". The dielectric zirconia embeds uncountable numbers of nanostructured metal ternary alloy islands of the material containing now NiPdD. The appearance is like a chocolate chip cookie on the nanoscale. The "chips" are hydrided palladium nickel metallic alloy embedded in a zirconium oxide dielectric matrix ("cookie").

The ZrO_2–(Pd Ni)D is prepared in a complicated process that begins by oxidizing a mixture of zirconium oxide surrounding metallic palladium, nickel, or Pd–Ni islands. This raw materials, PdZr oxide and ZrPdNi oxide, are available from Santoku Corporation (Japan) and Ames National Laboratory (Iowa). These are made as follows. First, there is made a co-melt (e.g. Zr (65%), Ni (30%), Pd (5%)) in a silica ampoule by the arc technique. The molten alloy is then dripped, and rapidly cooled, into a glassy form. This is done by taking the co-melt, adding the additives at this point, and the dropping the glassy material slowly between two water-cooled copper wheels, each with an angular velocity of ∼25 m/s. The sudden glassy freezing of the molten alloy produces an amorphous, metallic tinsel ribbon of size ∼0.5 mm × 2 to 20 mm × ca 0.1 mm thick. Thus, the majority of the Pd and Ni alloys appear as a foil; silvery-colored, shiny bright, and smooth. The next step is to bake the prenanostructure material in the air for 25–75 h at temperatures in the range of 270–390°C. Upon heating in air, the zirconium metal oxidizes into the oxidized ZrO_2 (zirconia) matrix which surrounds, encapsulates, and separates the NiPd alloy into 7–10 nm sized ferromagnetic nanostructured islands located and dispersed within the electrically insulating zirconia dielectric. The metallic ribbons are not magnetic prior to the air bake oxidation. However, they become magnetic, and semiconducting after the bake. We use several additional steps. For example, the size must be decreased further. This can be achieved by a rotary polishing drum (Thumler's Tumbler, Mod B). The rotary drum may take in the range of one to several days to achieve the size decrease, which must be carefully monitored. Flammability increases markedly as the size is decreased and finely powdered form appears; and therefore caution must be taken. Another series of steps are the backings of the prenanostructure material. On of these occurs over several days, at temperatures in the range of 270–390°C. Upon heating in air the zirconium metal oxidizes into the oxidized ZrO_2 (zirconia) matrix which surrounds, encapsulates, and separates the NiPd alloy into 10 nm sized ferromagnetic nanostructured islands in the insulating zirconia dielectric. The metallic ribbons are not magnetic prior to the air bake oxidation. They become magnetic, and semiconducting after the bake. If possible, the humidity should be removed because it can contribute to heterogeneity and inactive materials. Excessive temperatures should be avoided, because oxidation at 420°C for 24 h in air eliminates the smooth surface and makes the material inactive, as judged by in part to poor hydridation. The second baking is the vacuum bake at 200°C for 12–24 h. This is done to drive off any and all residual water vapor. Finally, the material can be very carefully ground in a mortar and pestle. The air bake temperature and time, and final proprietary dopants and processing appear to have critical importance.

The LANR nanostructured material is contained in the core volume (or chamber). The preloaded nanostructured material is placed into the hermetically sealed enclosure which is specially designed to withstand pressure, minimize

contamination, enable lock on of wires connecting to it. The enclosure is tightly fit because contamination is a potential problem, and because of the potential toxicity from the nanomaterial.

4. Experimental – Methods

The NANOR and the thermal control are at the center of much larger thermal mass in the calorimeter which is discussed in more detail in Ref. [1] (Fig. 2). The heat loss is the same for both the control and the component. One portion of the heat flow was measured by an Omega HFS Thin Film Heat flux sensor, with effort made to have significant heat flow go in one direction through the sensor.

The LANR preloaded, stabilized NANORs were driven by a high voltage circuit up to 3000 V rail voltage. The duty cycle was split with half going to a control portion consisting of a carefully controlled electrical DC pulse into an ohmic resistor which was used to thermally calibrate the calorimeter. These low power NANOR®-type components have been driven up to the two watt level.

The new controlled driving system uses pulse wave modulated microcomputer control of specialized very high voltage semiconductors linked to a current source driving system driving system coupled to the NANOR®-type LANR system. It provides an improved method of current control, enabling new activation, a new method of driving, an improved and better paradigm system and the ability to evolve paradigms. Furthermore, the system is excellent for preliminary tests to detect LANR activity, including for monitoring and/or examining changes in doping, and to examine different CF/LANR regions. We also employed a new series of LANR-directed light indicator outputs to define states which has been a matter of incredible utility and assistance almost every time the system and device has been used.

Basically, there are two levels of operation for NANOR LANR systems, low and high power. High power is useful for applications requiring larger amounts of power such as transportation, heating, and artificial organs. In this case, however, low power is used for several reasons including to facilitate the rapid time constant, and because this is for demonstration and teaching purposes. The new controlled driving system at low power was also very useful to more closely examine LANR and other systems for their activity, linearity, time-invariance, and even the impact of additives.

The instantaneous power gain (power amplification factor (non-dimensional)) is defined as $P_{\text{out}}/P_{\text{in}}$. The energy is calibrated by at least one electrical joule control (ohmic resistor) used frequently, and with time integration for additional validation. The excess energy, when present, is defined as ($P_{\text{output}} - P_{\text{input}}$) * time. The amount of output energy is determined from the heat released producing a temperature rise, which is then compared to the input energy. Data is taken from voltage, current, temperatures at multiple sites of the solution, and outside of the cell, and even as a 4-terminal measurement of the NANOR's internal electrical conductivity. Data acquisition has all temperature and electric measurements sampled at data rates of 0.20–1 Hz, with 24^{+} bit resolution (e.g. Measurement Computing (MA) USB-2416, or a Omega OMB-DaqTemp or equivalent; voltage accuracy $0.015^{\pm 0.005}$ V, temperature accuracy <0.6°C). All connections are isolated when possible, including where possible with Keithley electrometers, or their equivalent, for computer isolation. All leads are covered with dry, electrically insulating tubes, such as medical grade silicone, Teflon, and similar materials, used to electrically isolate wires. To minimize quantization noise, if necessary, 1 min moving averages may be used for some signals. The noise power of the calorimeter is in the range of ~1–30 mW. The noise power of the Keithley current sources is generally ~10 nW. Input power is defined as $V^{*}\ I$. There is no thermoneutral correction in denominator. Therefore, the observed power is a lower limit.

It is a long, expensive, arduous, effort to prepare these devices. The preloading of the nanostructured material is begun after preparation to the extent previously reported. This preloading system has achieved calculated loadings of 90 to >130%, with impressive results of excess heat over months at modest input power levels. The production of the preloaded core material involves preparation, production, proprietary pretreatment, loading, postloading treatment, activation, and then adding the final structural elements, including holder and electrodes. These are assembled to create the complete preloaded LANR nanomaterial package.

5. Results

It is clear that these preloaded nanostructured CF/LANR quantum electronic devices are very useful. The development of a more reproducible nanostructured CF/LANR quantum electronic device has not been easy, and has directly been linked to improved material, and avoidance of low-threshold breakdown states and quenching tendencies. Electrically, the response is complex. There are complicated polarization/transconduction phenomena including an "avalanche (transconduction electrical breakdown) effect" which has a critical role in excess heat generation [4]. The zirconia dielectric matrix is insulating at low voltage and keeps the nanoscale metal islands electrically separated. It also prevents the aggregation of the islands. Each nanostructured island acts as a short circuit elements during electrical discharge. These allow deuterons to form a hyperdense state in each island, where the deuterons are able to be sufficiently close together. In addition, the nanomaterial lattice of Pd is expanded by Zr, and also, but less so, by the H and D. In the former, there are then also wrought other major changes by the oxidation of the Zr. We previously reported sudden changes of, and generally large, electrical impedances of such NANOR®-type devices containing nanostructured materials. Several were ∼3 mΩ when lower voltages were applied, but then as the voltage was increased to ∼24 V, the impedance suddenly decreased to very low values. It was shown theoretically that this sudden reduction can be attributed to an "avalanche effect" that is typical of the current–voltage behavior that occurs in Zener diodes, and noted that this NANOR device, in principle, could be used in similar applications where Zener diodes have been used (e.g., for stabilizing circuits against potential surges in applied power). Control of the breakdown states and quenching tendencies has been critical. The newer materials have had transsample impedances of ∼300 gΩ, creating several serious problems. Surmounted them has been difficult but of value.

First, these preloaded NANOR®-type LANR devices have significant high efficiency heat production, with significant improvement over all of their predecessors in sustained activity, including the highly successful metamaterial PHUSOR®-type of LANR device. At their core is the proprietary preloaded nanostructure material specially prepared by several new processing steps. As a result, they had a much higher energy gain, even compared to the 2003 demonstration unit (Energy gain 14.1 in 2012 vs an energy gain ∼2.7 in 2003). In fact, the current Series VI NANORs have had even higher gains (to beyond 30).

Second, these JET Energy Inc. devices are conveniently preloaded, mountable as easily activated LANR (CF) components into Integrated Circuits. They are a new generation of activated CF/LANR nanocomposite ZrO_2–PdNiD electronic devices.

In the case of the Series V and VI NANOR®s ((miniature preloaded CF/LANR devices), the activation the activation of this cold fusion reaction is, for the first time, separated from its loading at room temperature. In every other system known, Fleischmann and Pons, Arata, Miles, and the others, the loading has been tied to activation.

By contrast, in the case of the sixth generation NANOR®s, unlike the others, the preloaded devices can be simply electrically driven.

Third, combined with a surrounding calorimeter and a unique driving system whose design, driving configuration and implementations, in conjunction with the NANOR® have made portability of LANR to MIT, and elsewhere, possible. This has created two spin-offs. The first is that the proprietary microprocessor controlled system has also led to an evolving series of improved driving paradigms to qualitatively explore and then exploit loaded nanostructured, nanocomposite, and other materials including semiquantitatively examining them for usefulness, heat-production activity, linearity, time-invariance, and even the impact of additives and contaminants. The other has been the demonstrated superior operation through preloaded nanostructured LANR material and requisite driving configuration over months. This has been shown by low power open demonstration, including the 2012 Open Demonstration at MIT which ran from January 30, 2012 through mid May 2012 (Figs. 1, 3, 4).

The self-contained CF/LANR quantum electronic component, a two terminal NANOR® containing active ZrO_2–PdD nanostructured material at its core, showed energy gain during, and after, the January, 2012 IAP MIT Course on

CF/LANR. In this case, the mini-sized NANOR is a 6th generation CF/LANR device, and it is smaller than 2 cm, with less than 1 g of active material. However, this is actually a matter which is not *de minimus* because the LANR excess power density was more than 19,500 W/kg of nanostructured material. The preloaded NANOR®-type LANR device demonstrated an average energy gain (COP) of ∼14× (∼1412%) the input for a duration of several hours that it was observed during the MIT IAP course on the first day, and levels of that order continued.

Over several weeks, the CF/LANR quantum device demonstrated more reproducible, controllable, energy gain which ranged generally from 5 to 16 (14.1 while the course was ongoing). The NANOR®-type preloaded LANR device openly demonstrated features include its convenient size (much smaller) and its superior handling properties which enable unique portability, and transportability. Like its 2003 (ICCF-10) predecessor demonstration, this preloaded NANOR®-type LANR device also showed excess energy and also further improvements of decreased size, decreased response time, improved and dual diagnostics, and increased total output energy density. The set-up was designed to run at low power input levels to increase the safety at the educational institution for its multi month-long stay at MIT. A range of experiments were conducted examining the impact of various driving sequences, and the NANOR® continued to produce excess energy, confirmed by daily calibrations. That system had parallel diagnostics including calorimetry, input-power-normalized ΔT, and focused heat flow measurement, and several calibrations. One of the calibrations included an ohmic (thermal) control located next to the NANOR, used to ascertain activity. To enable demonstrations at MIT for the NANOR system, including in the MIT IAP class where multiple experiments had to be shown to classes extending over times of 2 h, a specialized heat flow semiquantitative analyzer was specially developed. The heat which this preloaded NANOR®-type LANR device demonstrated was monitored three ways by three independent systems for semiquantitative measurement of the energy produced. Furthermore, the output of the NANOR® is compared to an ohmic control. First, the energy produced is instantaneously and kinematically determined by the ratio of the input power normalized temperature increase, called by the symbol '$\Delta T/P_{\text{in}}$' referring to the increase of temperature (ΔT), divided by the input electrical power (P_{in}). Second, it is also instantaneously and kinematically evaluated over a wide area by the ratio of the input power normalized heat flow leaving it, called by the symbol 'HF/P_{in}' referring to the heat flow (HF) divided by the input electrical power (P_{in}). Third, it is examined by calorimetry, calibrated by the thermal ohmic control, and confirmed by long-term time integration. These three methods of verification are pooled to derive very useful information, semiquantitatively ascertain energy produced, and infer activity.

Figures 1,3,4 show this entirely new, more reproducible, much more powerful configuration of clean, efficient energy production from several points of view. The figures include raw data and derived information from the runs which show conclusively LANR excess energy heralded by calorimetry and by input power normalized incremental temperature (ΔT) changes. These graphs shows a small portion of the collected data and derived information which was actually collected and analyzed by the class, and later in a four month interval.

Figure 1 is set of curves which plot the temperature rise (ΔT in °C) of the preloaded NANOR®-type LANR device and the ohmic control normalized to input electrical power. The NANOR® device received more than 10, and the ohmic control received five, levels of input electrical power. Each is shown with its thermal output response to its electrical input. Figure 1 presents the differential temperature rise normalized to input electrical power for the preloaded NANOR®, for the case with no input power ("Background"), and for the case of input to the ohmic thermal control, located at the core. The x-axis represents time, and each count represents 7 s. The y-axis on the left-hand side represents electrical input power in watts. Each of the outputs is read off of the right-hand side. The y-axis on the right-hand side represents the amount of temperature rise (differential temperature increase) normalized (that is, divided by) to the electrical input power. The units of this axis are in °C/W. Calibration pulses, used for accuracy and precisions checks of voltages and currents, are also shown. Compare the ΔT output normalized to input power for preloaded NANOR®-type LANR device to the thermal (ohmic) control. Observe that despite lower input electrical

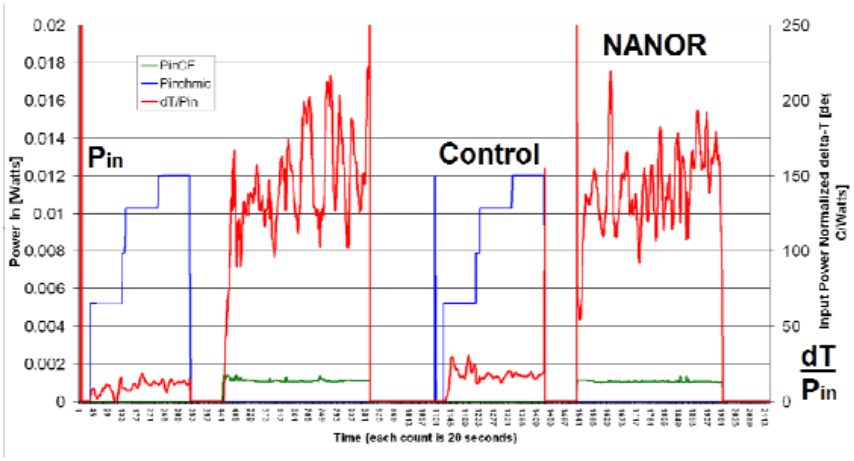

Figure 3. Input Power and Resulting Output Temperature rise (normalized to input electrical power) of a self-contained CF/LANR quantum electronic component, a Series VI two terminal NANOR®-type device containing active preloaded ZrO_2/PdiD nanostructured material at its core. These curves plot the temperature rise normalized to input electrical power.

power to the NANOR®, the temperature rise normalized to input electrical power observed in the core was higher than expected, as compared to the ohmic control. Note the active preloaded LANR quantum electronic device again clearly shows significant improvement in thermal output, here input-power-normalized compared to a standard ohmic control (a carbon composition resistor). Figure 1 heralds the excess energy achieved by the Series V NANOR® type of LANR device. It can be seen that the input power normalized delta-measurements suggests strongly the presence of excess heat.

Figure 3 shows the excess energy achieved by a slightly different type of self-contained CF/LANR quantum electronic component. This Series VI, preloaded, two terminal NANOR®-type device contained active preloaded ZrO_2/PdD nanostructured material at its core. These curves plot the temperature rise normalized to input electrical power. It can be seen that the input power normalized delta-measurements suggests strongly the presence of excess heat.

Figure 3 is set of curves which plot the temperature rise (ΔT in °C) of the preloaded NANOR®-type LANR device and the ohmic control normalized to input electrical power. The NANOR® device received a single level of electrical input power and the ohmic control received three levels of input electrical power. Each is shown with its thermal output response to its electrical input. Figure 3 presents the differential temperature rise normalized to input electrical power for the preloaded NANOR®, for the case with no input power ("Background"), and for the case of input to the ohmic thermal control, located at the core. The x-axis represents time, and each count represents 20 s. The y-axis on the left-hand side represents electrical input power in watts. Each of the outputs is read off of the right-hand side. The y-axis on the right-hand side represents the amount of temperature rise (differential temperature increase) normalized (that is, divided by) to the electrical input power. The units of this axis are in °/W. Calibration pulses, used for accuracy and precisions checks of voltages and currents, are also shown.

Compare the ΔT output normalized to input power for preloaded NANOR®-type LANR device to the thermal (ohmic) control. Observe that despite lower input electrical power to the NANOR®, the temperature rise normalized to input electrical power observed in the core was higher than expected, as compared to the ohmic control. Attention is

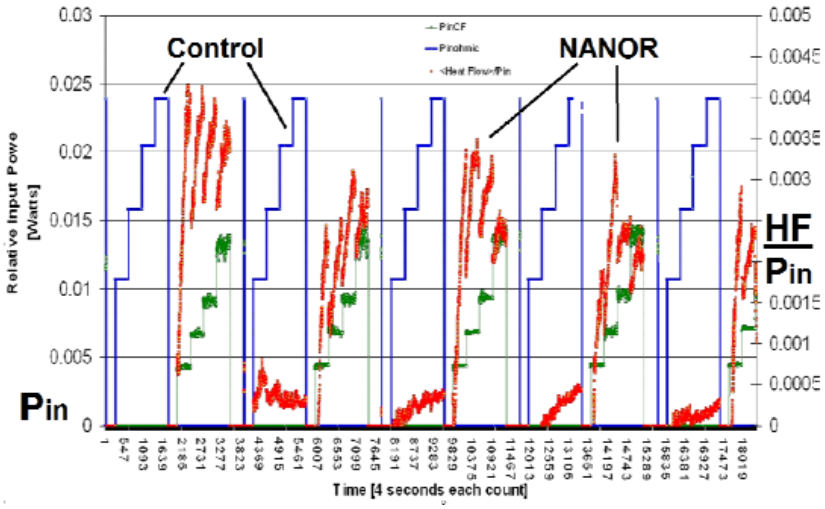

Figure 4. Input Power and Output Heat Flow normalized to input electrical power of a self-contained CF/LANR quantum electronic component 6-33.

directed to the fact that the active preloaded LANR quantum electronic device again clearly shows significant improvement in thermal output, here input-power-normalized compared to a standard ohmic control (a carbon composition resistor).

Figure 3 heralds the excess energy achieved by the Series V NANOR® type of LANR device. It can be seen that the input power normalized delta-measurements suggests strongly the presence of excess heat.

Figure 4 is set of curves which plot the heat flow, normalized to input electrical power, leaving the system while driving the preloaded NANOR®-type LANR device and the ohmic control at four different electrical input powers. The heat flow is in response to the electrical input. The figure presents the output heat flow for the preloaded NANOR®, for the case with no input, and for the ohmic thermal control, located at the calorimeter's core. In Fig. 4, the x-axis represents time, and each count represents 4 s. The y-axis on the left-hand side represents the electrical input power in watts. The y-axis on the right-hand side represents the Heat Flow output normalized (that is, divided by) to the electrical input power. Calibration pulses, used for accuracy and precisions checks of voltages and currents, are also shown. In Fig. 4, compare the output heat flow normalized to input power for NANOR®-type LANR device to that for the thermal (ohmic) control. The long term heat flow measurements (using calibrated devices) confirm the presence of excess energy, and validate the other measurements.

It can be seen that despite lower input electrical power to the NANOR®, the heat flow out in response, normalized to input electrical power observed in the core, was higher than expected, as compared to the ohmic control – especially at lower input power levels. The response of the NANOR®-type LANR device is consistent with very efficient energy production, with the energy output as heat. The changes of the output with input power is consistent with the optimal operating point manifold of the LANR material. Therefore, the figure heralds the significant excess energy coming from, the preloaded NANOR®-type of LANR device.

Attention is directed to the fact that the active preloaded LANR quantum electronic device clearly again shows significant improvement in energy generated compared to a standard ohmic control (a carbon composition resistor) by

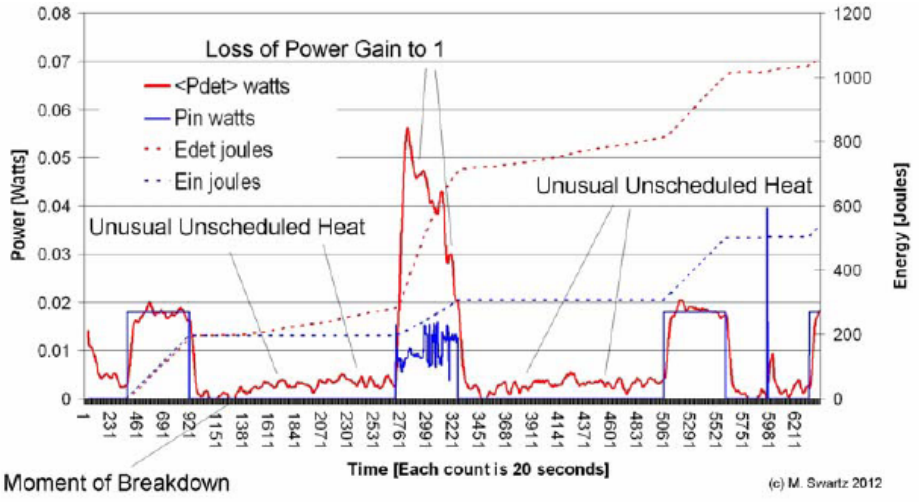

Figure 5. Electrical Input Power and Output Calorimetric response of a se NANOR®-type of CF/LANR quantum electronic component and the Catastrophic loss resulting in loss of excess energy.

this method, too, using heat flow. This information corroborates the marked and substantive incremental increase in energy output as heat for the preloaded Series VI NANOR®-type of LANR device.

Figure 5 is set of curves showing that under some conditions the NANOR® can actually catastrophically lose its excess energy producing properties becoming the exact equivalent of the ohmic control, and under some conditions creating distinguishing features in the calorimetry. Figure 5 shows curves which plot the electrical input power, at one input power level each to the preloaded NANOR®-type LANR device and the ohmic control, and the calorimetric responses of both.

The x-axis represents time, and each count represents 20 s. The$y$-axis on the left-hand side represents electrical input power in watts. The y-axis on the right-hand side represents the amount of energy released. The units of this axis are in joules. The figure shows the input, and the calorimetry, of preloaded NANOR® along with that for the ohmic thermal control used to calibrate the system. Those calibration pulses, used for accuracy and precisions checks of voltages and currents and time, are also shown. The inputs to the thermal ohmic control, followed by the preloaded NANOR®-type device, are shown, as are the calibrated calorimetric outputs for both.

Each of the outputs is read off on the right-hand side. The latter curves represent time integration to determine total energy. They thus rule out energy storage, chemical sources of the induced heat, and other sources of possible false positives. Compare the output for NANOR®-type LANR device to the thermal (ohmic) control. As can be seen, this semiquantitative calorimetry, itself calibrated by thermal waveform reconstruction, was consistent with excess heat being produced only during energy transfer to the NANOR®-type LANR device.

Notice that the active preloaded LANR quantum electronic device clearly shows significant improvement in thermal output compared to a standard ohmic control (a carbon composition resistor), however, in this case, there is instability in electrical input, at which time the excess energy produced by the device falls precipitously until the efficiency falls toward the equal to that of an ohmic thermal resistor (i.e. 100%). Note also that there was a sudden leakage of D from preloaded NANOR®-type LANR device with the “candle meltdown”-signature and the appearance of excess energy

from the exogenous nanostructure material. This refers only to the "melted candle"-shape of the temperature curve. This breakdown is the reason for the importance of the hermetic shields and the careful control via the sketch-driver system. It is also consistent with the catastrophic active media (CAM) theory of LANR/CF [19,20]. The graph is representative of the NANOR®-type of CF/LANR technology, and its shows quite clearly demonstrated over unity thermal output power from the NANOR® until the catastrophic event.

6. Conclusion

In summary, most importantly, for these NANOR®-type CF/LANR devices, the semiquantitatively measured output energy *is* a significant energy gain. This has always been a goal post for cold fusion, and one which so far remains beyond the realm for hot fusion on Earth by engineering means. As importantly, for these NANOR®-type CF/LANR devices, the activation of this cold fusion reaction is, for the first time, separated from its loading. at room temperature. Furthermore, the uniqueness of the preloaded LANR nanostructured material-device includes, beyond its high LANR activity, and its preloaded convenient nature, includes its dryness, its precise containment, and its easy portability. It begins a new generation of CF/LANR nanostructured materials and devices.

The present device and driving technology have provided high-efficiency preloaded energy-, heat-, and product-producing devices which can be electrically driven and has provided a method of improved activation and reproducibility for controlling lattice assisted reactions and their generated products using nanostructured, nanocomposite, and other materials.

Preloaded CF/LANR nanocomposite materials in CF/LANR Electronic Devices do have usefulness today and tomorrow. Today, they can be clearly examined with this system for demonstrations of their CF/LANR activity, linearity, time-invariance, and the impact of additives. For example, the present device, and controlling/driving system provided a reliable low power, high-efficiency (compared to an ohmic control; i.e. 100%) energy production device for demonstration and teaching purposes of size smaller than a centimeter, with an active site weight of less than 100 milligram.

The preloaded nanostructured LANR material and accompanying controller and driver shown at MIT was a successful (second) open demonstration of CF/LANR heat production and energy conversion device. This again confirms LANR/CF.

This open demonstration over months has demonstrated that microprocessor controlled integrated circuits using LANR quantum optical devices containing preloaded nanostructured LANR material can be used as an effective very clean, highly efficient, energy production system, apparatus, and process. In addition, elsewhere, this driving and monitoring system was useful to easily convert conventional monitoring and conventional thermometry into fine calorimetry. Calorimetry and input-power-normalized ΔT were used to ascertain activity. For example, this system has been used to show the calorimetry of a nanostructured composite CF/LANR Device using twenty different levels of input. This method is similar to, but beyond, that suggested by Dr. Robert W. Bass [21]. After testing it, we have determined that it was highly useful, and now use it routinely, wherever possible.

We have run the component over a year with evanescent loss which is attributed to fuel loss, or redistribution, or inactivation (perhaps by reaction with another material). Whether they can be refueled or simply replaced, is under investigation. Going forward, preloaded LANR nanostructured materials and devices will also be useful for integrated circuits and other applications using a pre-activated nanostructured and other materials. These include high power, self-contained, microprocessor controlled, preloaded, energy production devices and systems enabling their activation for electronic, medical, space and avionic circuits, integrated circuit devices, and artificial intelligence systems.

Acknowledgements

The authors gratefully thank Peter Hagelstein, Alex Frank, Alan Weinberg, Allen Swartz, Charles Entenmann, Dennis Cravens, Dennis Letts, Brian Ahern, Jeff Driscoll, Larry Forsley, Pamela Mosier-Boss, Robert Smith, Robert Bass, and the late Talbot Chubb; and JET Energy and New Energy Foundation for support. PHUSOR® and NANOR®\are registered trademarks. NANOR®-type and PHUSOR®-type technologies, and other discussed IP herein, is protected by U.S. Patents D596724, D413659 and other patents pending.

References

[1] M. Swartz and P.L. Hagelstein, Demonstration of energy gain from a preloaded ZrO_2–PdD nanostructured CF/LANR quantum electronic device at MIT, *ICCF17,* 2012.
[2] M. Swartz, Survey of the observed excess energy and emissions in lattice assisted nuclear reactions, *J. Sci. Exploration* **23** (4) (2009) 419–436.
[3] M. Swartz, Excess power gain using high impedance and codepositional LANR devices monitored by calorimetry, heat flow, and paired stirling engines, *Proc. 14th Int. Conf. on Cold Fusion (ICCF-14)*, 10–15 August 2008, Washington, D.C., D.J. Nagel and M. Melich (Eds.), ISBN: 978–0–578-06694-3, 2010, p. 123.
[4] M. Swartz and G. Verner, Excess heat from low electrical conductivity heavy water spiral-wound Pd/D_2O/Pt and Pd/D_2O–PdCl2/Pt devices, *Condensed Matter Nuclear Science, Proc. ICCF-1*0, P. Hagelstein and S Chubb (Eds.), World Scientific, NJ, ISBN 981–256–564-6, 2006, pp. 29–44, 45–54.
[5] M. Swartz, The impact of heavy water (D_2O) on nickel-light water cold fusion systems, *Proc. the 9th Int. Conf. on Cold Fusion* (Condensed Matter Nuclear Science), Beijing, China, Xing Z. Li (Ed.), May 2002, pp. 335–342.
[6] M. Swartz, Impact of an applied magnetic field on the electrical impedance of a LANR device, Volume 4 JCMNS, Proc. of the March 2010, New Energy Technology Symposium held at the 239th American Chemical Society National Meeting and Exposition in San Francisco (2011).
[7] M. Swartz, , LANR Nanostructures and Metamaterials Driven at their Optimal Operating Point, 3rd Volume of the LANR/LENR Sourcebook, October 21, 2011
[8] M. Swartz and G. Verner, The Phusor®-type LANR cathode is a metamaterial creating deuteron flux for excess power gain, *Proc. the 14th Int. Conf. on Condensed Matter Nuclear Science and the 14th Int. Conf. on Cold Fusion (ICCF-14)*, 10–15 August 2008, Washington, D.C., ISBN: 978–0-578-06694-3, 2010, p. 458.
[9] M. Swartz, Optimal operating point manifolds in active, loaded palladium linked to three distinct physical regions, *Proc. of the 14th Int. Conf. on Condensed Matter Nuclear Science and the 14th Int. Conf. on Cold Fusion (ICCF-14)*, 10–15 August 2008, Washington, D.C., David J. Nagel and Michael E. Melich (Eds.), ISBN: 978–0–578-06694-3, 2010, p. 639.
[10] M. Swartz, Quasi-one-dimensional model of electrochemical loading of isotopic fuel into a metal, *Fusion Technol.* **22**(2) (1992) 296–300.
[11] M. Swartz, Consistency of the biphasic nature of excess enthalpy in solid state anomalous phenomena with the quasi-1-dimensional model of isotope loading into a material, *Fusion Technol.* **31** (1997) 63–74.
[12] M. Swartz, Codeposition of palladium and deuterium, *Fusion Technol.* **32** (1997) 126–130.
[13] M. Swartz, G. Verner and A.Weinberg, Non-thermal near-ir emission from high impedance and codeposition LANR devices, *Proc. the 14th Int. Conf. on Condensed Matter Nuclear Science and the 14th Int. Conf. on Cold Fusion (ICCF-14)*, 10–15 August 2008, Washington, D.C., ISBN: 978–0–578-06694-3, 2010, p. 343.
[14] M. Swartz and G. Verner, Bremsstrahlung in hot and cold fusion, *J New Energy* **3**(4) (1999) 90–101.
[15] M. Swartz, P.L. Hagelstein, G. Verner and K. Wright, Vacancy-phase nickel cathodes, Abstracts, ICCF7, 1997, p. 137.
[16] Y. Arata and Y.C. Zhang, Observation of anomalous heat release and helium-4 production from highly deuterated palladium fine particles, *Jpn. J. Appl. Phys.* **38** (Part 2, No. 7A) (1999) L774–L776.
[17] F.L. Tanzella and M.C.H. McKubre, Calorimetry of pulse electro-melting of PdD_x wires, *Proc ICCF15,* 2009, pp. 42–46
[18] F. Tanzella, J. Bao, M. McKubre and P.L. Hagelstein, Stimulation of metal deuteride wires at cryogenic temperatures, *J. Cond. Matter Nucl. Sci.* **8** (2012) 176–186.

[19] M. Swartz, Catastrophic active medium hypothesis of cold fusion, Vol. 4. *Proc. Fourth Int. Conf. on Cold Fusion* sponsored by EPRI and the Office of Naval Research (1994).
[20] M. Swartz, Hydrogen redistribution by catastrophic desorption in select transition metals, *J. New Energy* **1**(4) (1997) 26–33.
[21] R.W. Bass, Five frozen needles CF protocol, *J. New Energy* **6**(2) (2002) 30.